2025 Annual Meeting
Poster #163

Using Mesh Morphing and Reduced-Order Modeling to Quantify the Influence of Fault Geometry on Earthquake Dynamic Rupture

Gabrielle Hobson[1], Dave A. May[1] & Alice-Agnes Gabriel[1,2]
[1]Institute of Geophysics and Planetary Physics, University of California San Diego
[2]Ludwig-Maximilians-Universität München, Munich, Germany

MTMOD: Megathrust Modeling Framework
NSF-EAR 2121568
sites.utexas.edu/mtmod/
Quakeworx
SCEC Project 25259
NSF OAC-2311208

Motivation

- Natural faults have complex, non-planar geometries with rough surfaces.
- Fault geometries are challenging to constrain observationally, even if surface rupture expressions are observed.
- Earthquake dynamic rupture simulations rely on meshes that exactly conform to fault geometries.
- Assumed fault geometries in models should incorporate uncertainty.
- Quantifying model sensitivity to geometric variability remains challenging because:
  - I. The process of geometry model and mesh generation is time-consuming and often non-automated.
  - II. The parameter space to be explored is high-dimensional.
  - III. Dynamic rupture simulations may be computationally expensive.

⇒ We present a mesh morphing approach that applies geometric variations to a reference mesh while preserving mesh connectivity, enabling reduced order modeling and sensitivity analysis with respect to varying fault geometry.

The Mesh Morphing Method

- Mesh morphing takes a mesh $\boldsymbol{X}_M$ representing a geometry $\mathcal{G}_1$ and deforms (morphs) the mesh into a new configuration $\widehat{\boldsymbol{X}}_M$ representing a new geometry $\mathcal{G}_2$ [1].
- Displacements are prescribed for certain points and used to build a radial basis function (RBF) interpolant.
- The interpolant is evaluated at all mesh vertices, and the resulting displacements relocate the vertices to new positions.
- The mesh topology (including mesh connectivity) does not change.

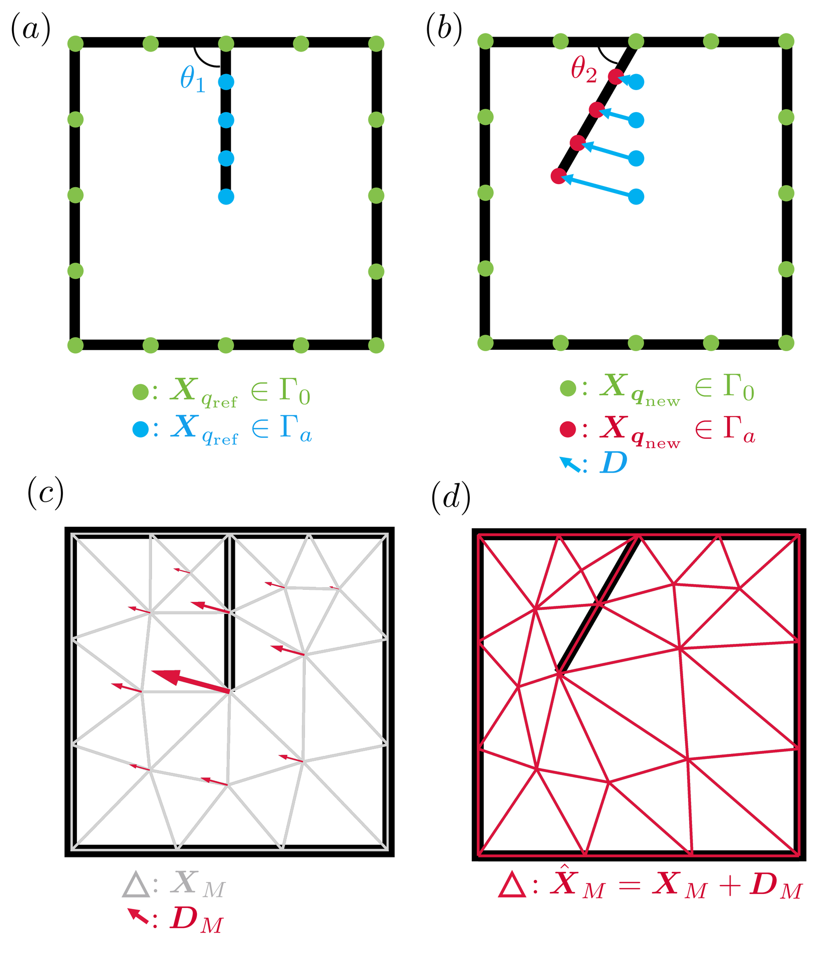

Figure 1. Illustration of the mesh morphing method. (a) The reference geometry, in black, as well as points $\boldsymbol{X}_{q_{\rm ref}}$ which lie on Γ_0, in green, and those which lie on Γ_a, in blue. (b) The new geometry, in black, as well as points $\boldsymbol{X}_{q_{\rm new}}$ which lie on Γ_0, in green, and those which lie on Γ_a, in blue. (c) the reference mesh in gray, with vertices $\boldsymbol{X}_M$, and the displacement applied to each vertex, $\boldsymbol{D}_M$. (d) The morphed mesh, $\widehat{\boldsymbol{X}}_M$.

Mesh Morphing Steps

1. Define a geometric parameter, $\boldsymbol{q} = (\theta)$ with reference value θ_1.
2. Assign boundaries or surfaces to have zero displacement (Γ_0) or non-zero displacement (Γ_a).
3. Define points $\mathbf{X}_{q_{\rm ref}}$ on the reference geometry boundaries.
4. Define points $\mathbf{X}_{q_{\rm new}}$ on boundaries of target geometries with $\boldsymbol{q}_{\rm new} = \theta_2, \theta_3 \ldots \theta_m$.
5. Compute displacement $\boldsymbol{D}$ between $\mathbf{X}_{q_{\rm ref}}$ and $\mathbf{X}_{q_{\rm new}}$.
6. Define an RBF interpolant F_{RBF} $(\boldsymbol{q}_{\rm new}, \boldsymbol{D})$ with weights $\underline{w}_F$.
7. Evaluate F_{RBF} at the desired $\theta_{\rm eval}$ value to obtain displacements $\boldsymbol{D}_j$.
8. Define a second interpolant G_{RBF} $(\mathbf{X}_{q_{\rm ref}}, \boldsymbol{D})$ with weights $\underline{w}_G$.
9. Evaluate G_{RBF} at the reference mesh vertices X_M to get displacements $\boldsymbol{D}_M$.
10. Add displacements to obtain morphed mesh, $\widehat{\boldsymbol{X}}_M = \boldsymbol{X}_M + \boldsymbol{D}_M$.
11. Check mesh validity and quality.

Example: Varying Fault Dip

- We demonstrate the application of mesh morphing to the SCEC/USGS TPV13-3D benchmark exercise [2], with dynamic rupture simulations performed using SeisSol [3].
- TPV13 features spontaneous rupture on a 2D planar normal fault at 60° dip, with supershear rupture, linear slip-weakening friction, and off-fault plasticity governed by a non-associative Drucker-Prager visco-plastic rheology.
- The reference mesh is generated using GMSH [4].

⇒ We morph the mesh to have fault dip angles between [40°, 80°] and we decrease the nucleation patch static friction coefficient from 0.54 to 0.48 to allow rupture on faults with dips in the range [50°, 70°].

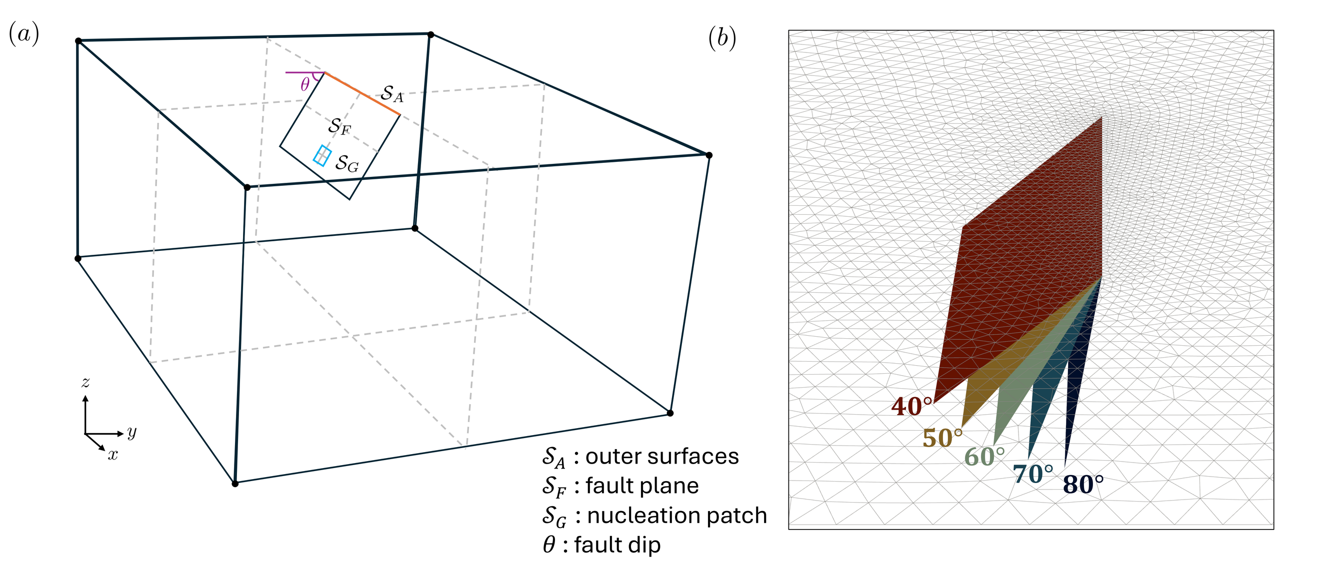

Figure 2. (a): the TPV13 geometry, with the fault trace in orange, the nucleation patch boundary in blue, and the fault dip in purple. (b): Fault planes for different θ, with the surface mesh shown as a gray wireframe.

Morphed Mesh Quality

- The reference mesh ($\theta = 60°$) is morphed to have a wide range of fault dip, $\theta \in [40°, 80°]$, while maintaining acceptable mesh quality.
- We generate meshes with matching dip angles for comparison using GMSH [4].
- The max distance between fault vertices in morphed and generated meshes is 140 - 150 m, with an RMS distance of 71 - 73 m.

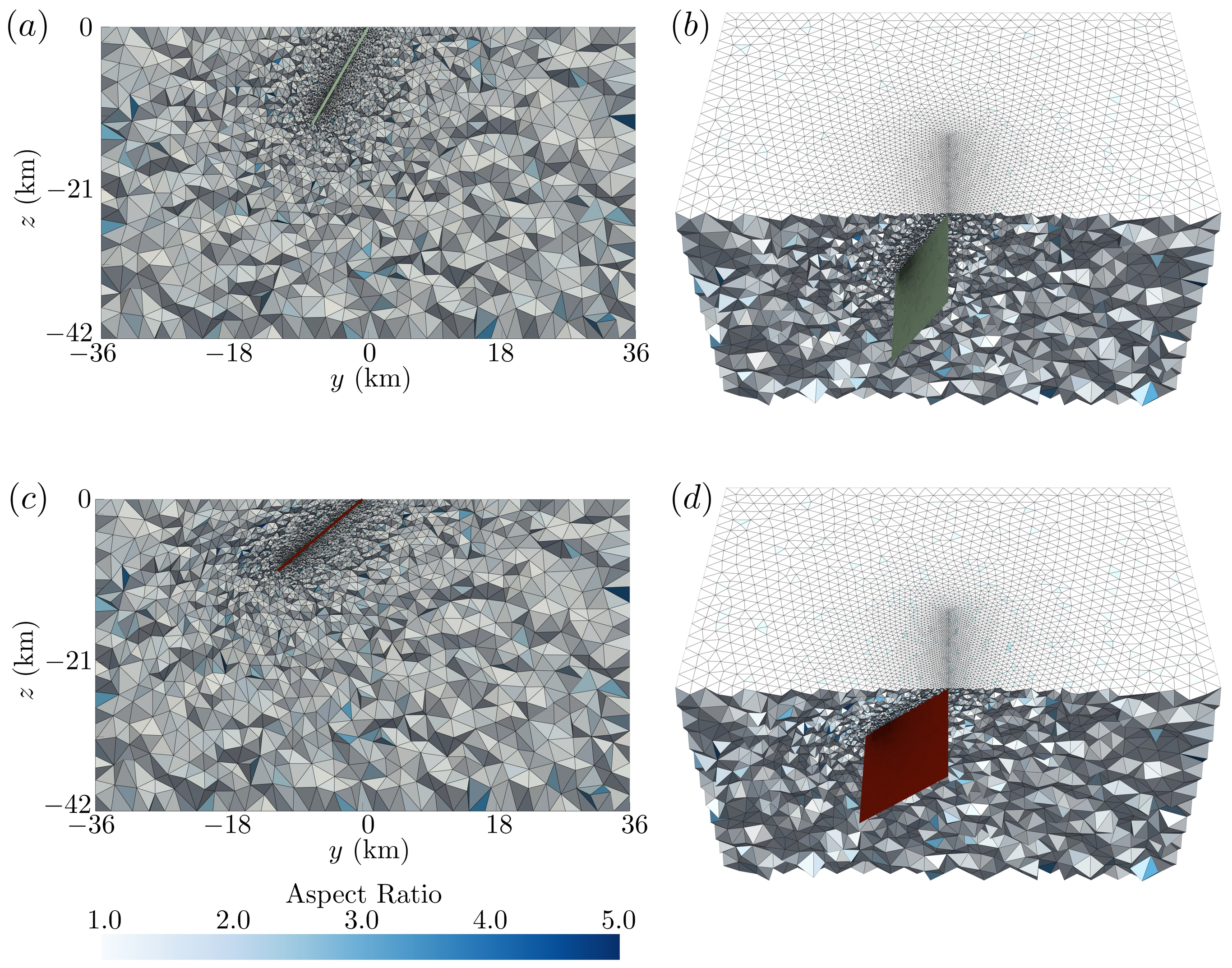

Figure 3. The reference mesh ($\theta = 60°$) shown from a side on view (a) and angled view (b). The morphed mesh with $\theta = 40°$ is shown in (c) and (d). Cells are colored by mesh quality based on the Aspect Ratio metric.

	Aspect Ratio		Scaled Jacobian		Min Angle (°)	
θ	Avg	Max	Avg	Min	Avg	Min
40°	1.6	6.4	0.6	0.11	48	9
50°	1.6	5.2	0.62	0.13	49	11
60°	1.5	5.1	0.63	0.15	49	11
70°	1.6	5.4	0.62	0.15	49	10
80°	1.6	5.4	0.62	0.15	49	10

Table 1. Mesh quality metrics for the full mesh volume as θ varies. The reference mesh is highlighted in grey.

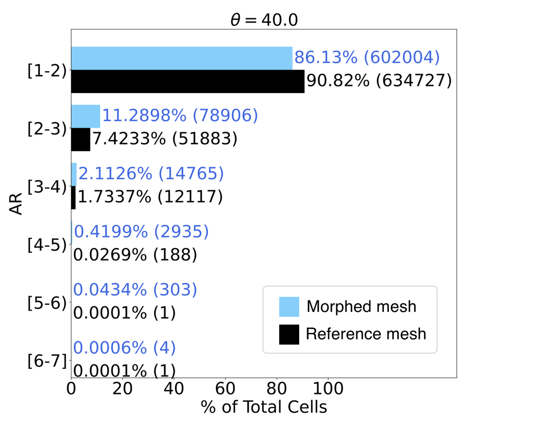

Figure 4. Ranges of aspect ratio values and the percent of mesh cells that fall within that range as θ varies.

Comparisons of Simulation Output

- We find good agreement when comparing both on-fault and off-fault output from SeisSol simulations run on morphed and generated meshes.
- Velocity components recorded at off-fault receivers agree strongly for v_y (horizontal, fault perpendicular) and v_z (vertical) components; differences in v_x (horizontal, fault parallel) have comparatively small magnitudes.
- Accumulated slip is slightly over-predicted at $t = 1$ s when using a morphed mesh (by 0.3 m/s), but agrees well at other time steps.

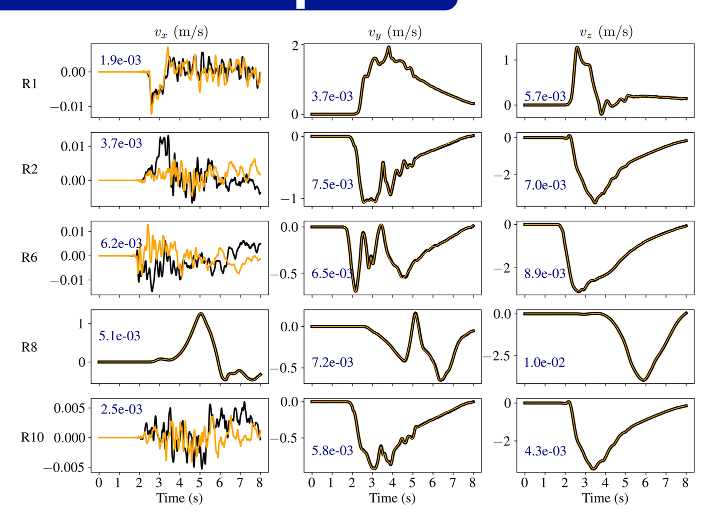

Figure 5. Velocity components at 5 off-fault receivers for $\theta = 50°$. Generated mesh output in black, morphed mesh output in orange, and RMSE values in blue.

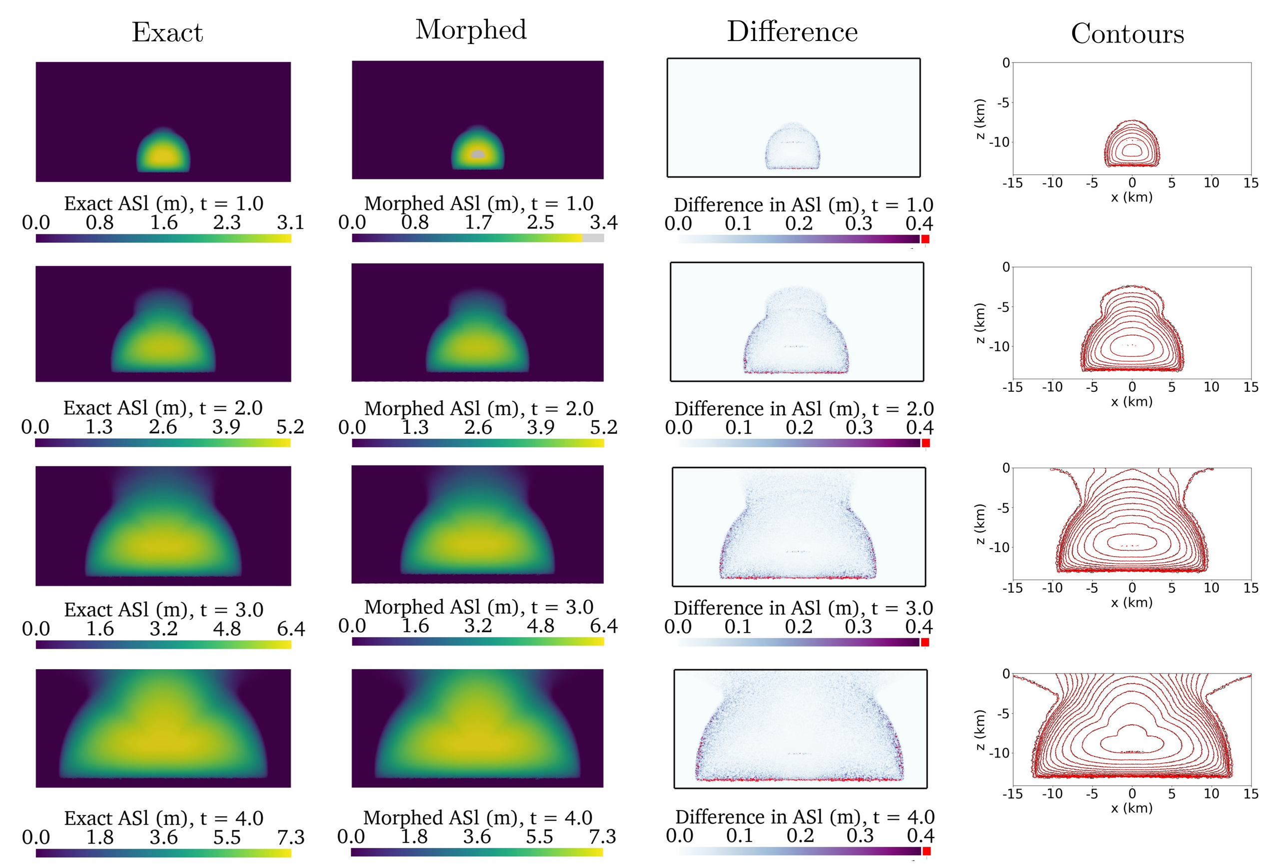

Figure 6. Accumulated slip (ASl) on the fault for $\theta = 70°$. Output from generated meshes (left) and morphed meshes (center left), and the absolute value of the difference (center right). To the right, contours drawn at 0.5 m intervals for generated (black) and morphed (red) output.

Reduced-Order Models for Dynamic Rupture

- The mesh morphing method preserves mesh connectivity during morphing, which allows us to apply data-driven, non-intrusive reduced-order modeling [5,6].
- We construct reduced-order models (ROMs) from dynamic rupture simulation output using the interpolated Proper Orthogonal Decomposition (iPOD) approach [7,8,9,10], which has recently been applied in several geophysical applications [11,12,13].
- The ROMs approximate simulation output and are highly efficient to evaluate, permitting robust global sensitivity analysis with respect to varying geometries.

Reduced-Order Model for Vertical Surface Displacement u_z

- ROM constructed using vertical surface displacement u_z at a given timestep from SeisSol simulations run on morphed meshes for $\theta = [50°, 51°, \ldots 69°, 70°]$.
- Leave-one-out cross-validation L_∞ error is 0.03-0.06 m at edge of parameter space, but within parameter interval it is < 0.01 m and typically < 0.005 m (or 0.1% of max u_z).

⇒ **3.15×10^4 s : Offline cost (walltime) to build ROM (SeisSol + iPOD)**
5×10^{-4} s : Online cost (walltime) to evaluate ROM
$10^8\times$: Speedup of ROM (once built) relative to SeisSol

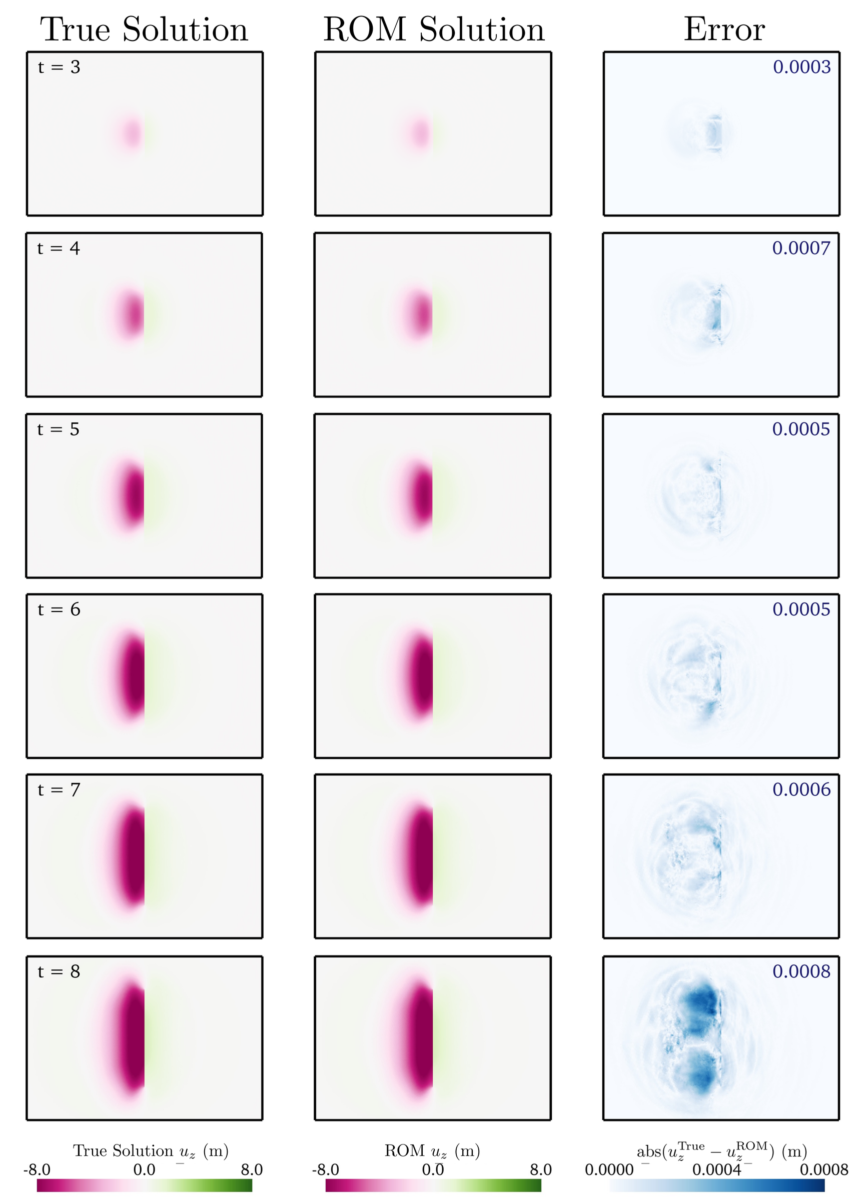

Figure 7. SeisSol output vs. reduced order model (ROM) approximations of the vertical ground displacement u_z for a fault dip of $\theta = 52.5°$, with max error in blue text.

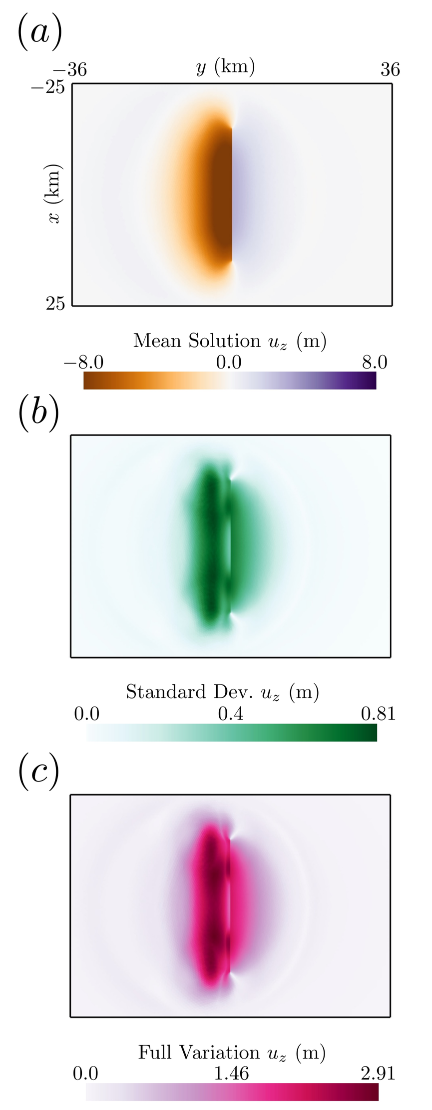

Figure 8. (a) Mean field, (b) standard deviation, and (c) maximum variability as fault dip varies, for vertical ground displacement u_z at simulation time $t = 8$ seconds.

Reduced-Order Model for Velocity Series History at Off-Fault Receivers

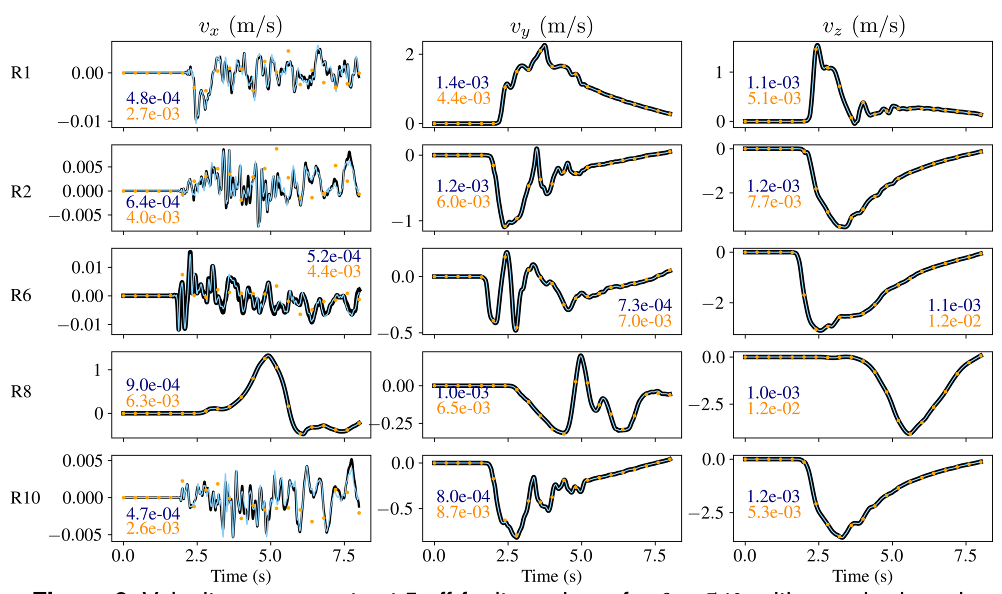

A unique ROM is built for each receiver.

3.15×10^4 s : Offline cost (walltime) to build ROM

5×10^{-5} s : Online cost (walltime) to evaluate ROM

$10^9\times$: Speedup of ROM (once built) relative to SeisSol

Figure 9. Velocity components at 5 off-fault receivers for $\theta = 54°$, with morphed mesh velocity in black, the ROM approximation in blue, and generated mesh velocity as orange points; RMSE between morphed mesh velocity and ROM approximation in dark blue text, and RMSE between generated mesh velocity and ROM approximation in orange text.

Summary

- We present a method for generating ensembles of geometrically varying meshes.
- We apply this method to meshes for 3D earthquake dynamic rupture simulations.
- We demonstrate using mesh morphing enabled reduced-order models to quantify the sensitivity of earthquake rupture to geometric variability by measuring the variation in vertical surface displacement as fault dip varies.

Outlook for complex fault systems:

- Fault networks with stepovers, branches, and/or intersecting faults.
- Dip angle, trace, curvature, and roughness of faults are geometric parameters of interest.
- Morphing non-intersecting faults is tractable; morphing intersecting faults is challenging, likely requiring successive morphs and limited geometric variation especially near intersections.

arXiv
Preprint available

[1] Sieger, Menzel, & Botsch (2014). *Engineering with Computers*, 30, 161– 174.
[2] Harris et al. (2018). *Seismological Research Letters*, 89(3), 1146-1162.
[3] Gabriel et al. (2025). Seissol. Zenodo. doi: 10.5281/zenodo.15685917
[4] Geuzaine & Remacle (2009). *Int. J. Num. Meth. Eng.,* 79(11), 1309-1331.
[5] Sirovich (1987). *Quarterly of Applied Mathematics*, 45(3), 561–571.
[6] Holmes et al. (2012). Cambridge University Press, Cambridge.
[7] Ly & Tran (2001). *Mathematical and Computer Modelling*, 33(1), 223-236.
[8] Bui-Thanh et al. (2003). In *21st AIAA Applied Aerodynamics Conference.*
[9] My-Ha et al. (2007). *Comp. & Fluids*, 36(3), 499-512.
[10] Walton et al. (2013). *Appl. Math. Modelling*, 37, 8930-8945.
[11] Rekoske et. al. (2023). *Journal of Geophysical Research: Solid Earth*, 128(8), e2023JB026975.
[12] Rekoske et al. (2025). *Geophysical Journal International,* 241(1), 526-548.
[13] Hobson & May (2025). *Geochem., Geophysics, Geosystems*, 26(5). e2024GC011937